Ab Initio Study of the Effects of Torsion Angles on Carbon-13 Nuclear Magnetic Resonance Chemical Shielding in *N*-Formyl-L-alanine Amide, *N*-Formyl-L-valine Amide, and Some Simple Model Compounds: Applications to Protein NMR Spectroscopy†

Angel C. de Dios and Eric Oldfield*

Contribution from the Department of Chemistry, University of Illinois at Urbana-Champaign, 505 South Mathews Avenue, Urbana, Illinois 61801

Received November 19, 1993®

Abstract: In order to understand better the origins of the chemical shift nonequivalencies observed in proteins due to folding, we have investigated the effects of torsion angles on ^{13}C nuclear magnetic resonance shielding in a series of compounds, using a gauge-including atomic orbital (GIAO) method. We regard the naturally occurring L-amino acids as ethane derivatives $C^{\beta}HABC^{\alpha}HCD$, and we have computed the effects of χ^1 ($HC^{\beta}C^{\alpha}H$) on C^{α}, C^{β} shielding in ethane, propane, 2-methylpropane, aminoethane, propanal, and 2-aminopropanal, as well as the effects of ϕ, ψ, and χ^1 torsion angles on C^{α}, C^{β} shielding in the peptide models *N*-formyl-L-alanine amide and *N*-formyl-L-valine amide. Our results show for the simpler model compounds that C^{α} substitution causes a much larger effect on C^{β} shielding (as a function of χ^1) than on C^{α} shielding. For the two peptide model compounds, ϕ, ψ torsions strongly affect C^{α}, C^{β} shielding, with the largest χ^1 effect being seen with valine C^{β}. These dependencies are discussed in relation to some of the chemical shift nonequivalencies due to folding observed in the ^{13}C NMR spectra of *Drosophila melanogaster* calmodulin and *Staphylococcal* nuclease.

Introduction

Although the existence of large chemical shift nonequivalencies due to folding has been observed in protein NMR spectra for some time,[1,2] it has only recently been demonstrated[3,4] that these chemical shift differences can be theoretically predicted. Such shielding computations for systems as large as proteins have been made feasible by treating the total shielding, σ_t, as composed of three parts:[5]

$$\sigma_t = \sigma_s + \sigma_e + \sigma_m \quad (1)$$

where σ_s represents the short-range or electronic component, σ_e is the shielding component due to electrostatic polarization of the electrons in the vicinity of the nucleus of interest, and σ_m is a magnetic contribution, arising from, for example, ring currents and bulk susceptibility effects, as well as the magnetic anisotropies arising from peptide and other carbonyl groups. By virtue of this partitioning, the hardware resources (i.e. disk space, memory, and computation time) required for *ab initio* calculations are greatly ameliorated due to the fact that only the evaluation of the short-range component, σ_s, requires atomic centers equipped with basis functions. The electrostatic contributions can be computed either by using a charge-field perturbation approach or via the shielding polarizabilities,[6] and the magnetic anisotropy terms can be adequately treated using a variety of (rapid) semiclassical methods.[7]

The first component, σ_s, contains the influences of local geometry (e.g. torsion angles, bond lengths, and bond angles), and on the basis of an initial analysis of the shielding of backbone carbon nuclei in these systems, it has been suggested[8] that the chemical shielding nonequivalences observed in proteins are primarily due to the effects of the torsion angles ϕ, ψ, and χ. Thus, a good approximation to the total shielding can usually be obtained simply by taking into account the dependencies of the shielding on these three torsion angles. Moreover, these structure–shielding correlations imply that it may be possible to deduce structural information from chemical shifts in proteins. However, this will only be possible if there are clearly-defined relationships between torsion angles and the observed chemical shifts. We thus report a detailed investigation of how torsion angles influence chemical shifts in peptides as well as some simpler model compounds.

In this work, we explore the shielding dependencies of the C^{α} and C^{β} carbons in a series of variously substituted ethanes $C^{\beta}HABC^{\alpha}HCD$, where C^{β} and C^{α} correspond to the α and β carbon atoms in amino acids (or their peptide model compounds). The following series of compounds, ranging from ethane to heptapeptides, have been investigated in detail in this work: ethane, propane, 2-methylpropane, aminoethane, propanal, 2-aminopropanal, *N*-formyl-L-alanine amide, *N*-formyl-L-valine amide, HCO-Gly-L-Ala-Gly-NH_2, HCO-Gly-Gly-L-Ala-Gly-Gly-NH_2, and HCO-Gly-Gly-Gly-L-Ala-Gly-Gly-Gly-NH_2. The tri-, penta-, and heptapeptide systems were investigated in both helical and sheet conformations in order to evaluate the longer range contributions to shielding. The results obtained help us gain insight into how torsion angles affect chemical shifts and, in turn, serve as a guide for future calculations of shielding surfaces of other amino acids. We find, in particular, that C^{α}, C^{β} chemical

† This work was supported by the National Institutes of Health (Grant HL-19481) and by an equipment award from the International Business Machines Corp. Shared University Research Equipment Program.
* Abstract published in *Advance ACS Abstracts*, May 15, 1994.

(1) McDonald, C. C.; Phillips, W. D. *J. Am. Chem. Soc.* **1969**, *91*, 1513.
(2) Allerhand, A.; Childers, R. F.; Oldfield, E. *Biochemistry* **1973**, *12*, 1335.
(3) de Dios, A. C.; Pearson, J. G.; Oldfield, E. *Science* **1993**, *260*, 1491.
(4) Laws, D. D.; de Dios, A. C.; Oldfield, E. *J. Biomol. NMR* **1993**, *3*, 607.
(5) de Dios, A. C.; Oldfield, E. *Chem. Phys. Lett.* **1993**, *205*, 108.
(6) Augspurger, J. D.; Dykstra, C. E. *J. Phys. Chem.* **1991**, *95*, 9230. Augspurger, J. D.; de Dios, A. C.; Oldfield, E.; Dykstra, C. E. *Chem. Phys. Lett.* **1993**, *213*, 211. Augspurger, J.; Pearson, J.; Oldfield, E.; Dykstra, C. E.; Park, K. D.; Schwartz, D. *J. Magn. Reson.* **1992**, *100*, 342.
(7) Johnson, C. E.; Bovey, E. A. *J. Chem. Phys.* **1958**, *29*, 1012.
(8) de Dios, A. C.; Pearson, J. G.; Oldfield, E. *J. Am. Chem. Soc.* **1993**, *115*, 9768.

0002-7863/94/1516-5307$04.50/0

Table 1. Nuclei Whose Shielding Has Been Calculated as a Function of the Torsion Angle

molecule	nuclei	torsion angle	range
ethane (H_3CCH_3)	C	H–C–C–H	0°–60°
propane ($H_3CCH_2CH_3$)	C^1,C^2	H–C^1–C^2–C^3	0°–120°
isobutane ($(CH_3)_2CHCH_3$)	C^1,C^2	H–C^1–C^2–H	0°–120°
ethylamine ($H_2NCH_2CH_3$)	C^1,C^2	N–C^1–C^2–H	0°–120°
propanal ($OHCCH_2CH_3$)	C^2,C^3	C^1–C^2–C^3–H	0°–120°
(*S*)-2-aminopropanal ($OHCCH(NH_2)CH_3$)	C^2,C^3	C^1–C^2–C^3–H	0°–120°
formylalanine amide ($OHCNHCH(CH_3)CONH_2$)			
sheet 1 ($\phi = -140°, \psi = 140°$)	C^α, C^β	H^α–C^α–C^β–H^β	0°–120°
sheet 2 ($\phi = -71°, \psi = 140°$)	C^α,C^β	H^α–C^α–C^β–H^β	0°–120°
helix ($\phi = -55°, \psi = -55°$)	C^α,C^β	H^α–C^α–C^β–H^β	0°–120°
turn ($\phi = 55°, \psi = 50°$)	C^α,C^β	H^α–C^α–C^β–H^β	0°–120°
formylvaline amide ($OHCNHCH(CH(CH_3)_2)CONH_2$)			
sheet ($\phi = -136°, \psi = 143°$)	C^α,C^β	H^α–C^α–C^β–H^β	−180°–180°
helix ($\phi = -55°, \psi = -55°$)	C^α,C^β	H^α–C^α–C^β–H^β	−180°–180°

shifts for alanine and valine residues in a *Drosophila* calmodulin can be predicted with good accuracy (rmsd of ~2 ppm for a total chemical shift range of ~50 ppm), and given ϕ, ψ, the shielding results give useful information about χ_1 also.

Computational Aspects

SCF and shielding calculations were carried out by using the TEXAS 90 program of Pulay and co-workers,[9,10] which implements the GIAO (gauge-including atomic orbital) method[11] for shielding computation. All calculations were performed on a cluster of IBM RISC/6000 computers (International Business Machines Corp., Austin, TX) equipped with a total of 0.4 GB of RAM and 40 GB of disk space and operating at a peak theoretical speed of 1.0 Gflop. The basis set used was the 6-311G basis of Pople and co-workers,[12] augmented with two sets of d-type polarization functions on the heavy atoms, two sets of p-type functions on the hydrogens, and diffuse functions on all atoms, 6-311++G(2d,2p). The geometries at the staggered or *trans*-conformations were obtained via extensive energy minimization (>10 000 steps) using the Discover Program (Biosym Technologies, San Diego, CA). The shieldings of the carbons in ethane were computed at 15° increments of the dihedral angle (H–C–C–H), from the eclipsed to the staggered conformation, keeping all the other internal coordinates fixed. These calculations were then repeated using SCF level optimization of all coordinates at each dihedral angle.

Shielding calculations were also performed on the following molecules: propane, 2-methylpropane, aminoethane, propanal, 2-aminopropanal, formylalanine amide, and formylvaline amide. The structures, dihedral angle ranges, and nuclei of interest for these molecules are shown in Table 1. For formylalanine amide and formylvaline amide, an attenuated basis set was used,[3,13] and as shown in Table 1, several conformations were studied, representative of sheets and helices. Due to the loss of symmetry brought about by the side chain in valine, the staggered conformers become unique. The χ^1 dependence of the C^α and C^β shieldings in the valine model fragment therefore necessitated evaluation of ϕ–ψ shielding surfaces at the three different staggered conformations, $\chi^1 = 180°$, 60°, and −60°, in regions of ϕ,ψ space which are populated by most valine residues in proteins. Finally, to investigate the effects of longer range contributions to shielding, we investigated three model peptides, HCO-Gly-Ala-Gly-NH_2, HCO-Gly-Gly-Ala-Gly-Gly-NH_2, and HCO-Gly-Gly-Gly-Ala-Gly-Gly-Gly-NH_2, using representative sheet and helical torsion angles. Since these fragments are quite large, a uniform (6-31G) basis was used. The torsion angles of the heptapeptide are shown in Table 2, with the smaller residues being constructed via removal of the appropriate numbet of glycine residues.

Results and Discussion

A number of previous workers have investigated the effects of dihedral angles on shielding. For example, Barfield and Yamamura[14] used the IGLO method[15] to describe ^{13}C shielding dependencies at the α-, β-, and γ-positions of aliphatic and alicyclic hydrocarbons, and more recently, Webb and co-workers have reported GIAO results for *n*-octane[16] aimed at reproducing the γ-*gauche* effect first observed by Grant and co-workers.[17] Webb's results show that the γ-position in a *gauche* conformation is ~3 ppm more shielded compared to the *trans*-conformation, somewhat smaller than the experimental value of ~5 ppm. The α- and β-positions were likewise found to be more shielded in the *gauche*-conformation.[16,18] Here, it is important to note that in these calculations the bond lengths and bond angles were optimized for each fixed dihedral angle. Barfield has also reported similar IGLO calculations for γ-positions in various hydrocarbons,[19] and as in Webb's work, the geometrical parameters were optimized at each given dihedral angle.

Table 2. Torsion Angles (deg) for HCO-Gly^1-Gly^2-Gly^3-Ala^4-Gly^5-Gly^6-Gly^7-NH_2

	helix		sheet	
residue	ϕ	ψ	ϕ	ψ
Gly^1	−41	−55	−71	65
Gly^2	−54	−49	−70	64
Gly^3	−58	−51	−70	65
Ala^4	**−53**	**−51**	**−140**	**140**
Gly^5	−51	−54	−70	65
Gly^6	−50	−49	−70	64
Gly^7	−57	−45	−70	63

Since we are interested in computing shielding surfaces for the heavy atoms in each of the 20 naturally occurring amino acids (≫10^4 shielding calculations), it is clearly of some interest to decide at an early date whether or not it is absolutely essential to use *ab initio* structure optimization techniques in order to be able to successfully predict experimental chemical shifts and their torsional dependencies, and ethane provides the simplest test case. Figure 1 shows our results for ethane, and it can be seen that the effects of fully relaxing the other geometrical parameters are quite negligible. This result is in agreement with that obtained by Kutzelnigg and co-workers using the IGLO method.[20] Chesnut and co-workers[21] have also studied the effects of torsion on the ^{13}C chemical shift in ethane using the GIAO method but using

(9) Pulay, P.; Wolinski, K.; Hinton, J. F. *The Texas Program*; University of Arkansas: Fayetteville, AR, 1991.
(10) Wolinski, K.; Hinton, J. F.; Pulay, P. *J. Am. Chem. Soc.* **1990**, *112*, 8251.
(11) Ditchfield, R. *J. Chem. Phys.* **1972**, *56*, 5688.
(12) Krishnan, R.; Binkley, J. S.; Seeger, R.; Pople, J. A. *J. Chem. Phys.* **1980**, *72*, 8251.
(13) Chesnut, D. B.; Moore, K. D. *J. Comput. Chem.* **1989**, *10*, 648.
(14) Barfield, M.; Yamamura, S. H. *J. Am. Chem. Soc.* **1990**, *112*, 4747.
(15) Schindler, M.; Kutzelnigg, W. *J. Chem. Phys.* **1982**, *76*, 1919.
(16) Kurosu, H.; Ando, I.; Webb, G. A. *Magn. Reson. Chem.* **1993**, *31*, 399.
(17) Paul, E. G.; Grant, D. M. *J. Am. Chem. Soc.* **1963**, *85*, 1701.
(18) Anet, F. A. L.; Cheng, A. K. *J. Am. Chem. Soc.* **1975**, *97*, 2420.
(19) Barfield, M. In *Nuclear Magnetic Shieldings and Molecular Structure*; Tossell, J. A., Ed.; NATO ASI Series C, Vol. 386; Kluwer: Dordrecht, The Netherlands, 1993; p 523.
(20) Kutzelnigg, W.; van Wullen, C.; Fleischer, U.; Franke, R.; van Mourik, T. In *Nuclear Magnetic Shieldings and Molecular Structure*, Tossell, J. A., Ed.; NATO ASI Series C, Vol. 386; Kluwer: Dordrecht, The Netherlands, 1993; p 141.
(21) Chesnut, D. B.; Wright, D. W.; Macphail, R. A. *Chem. Phys. Lett.* **1988**, *151*, 415.

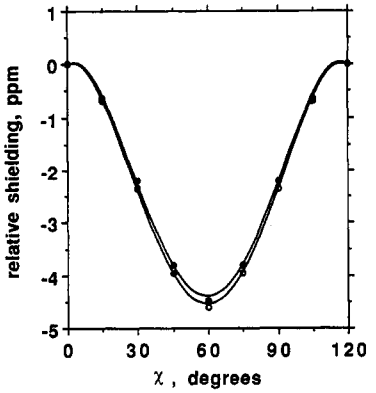

Figure 1. Calculated ^{13}C shieldings in ethane as a function of the torsion angle, χ. (○) Only χ was varied while the other structural parameters were fixed. (●) Fully relaxed structural parameters were used at each χ value.

a smaller basis (6-311G(1d) for C and 4-31G for H) for both shielding calculations and geometry optimization. The torsional effect on the shielding determined by Chesnut et al.[21] was then extracted via corrections using shielding derivatives with respect to bond length and angle changes, and these workers concluded that nearly 90% of the change in isotropic shielding was attributed to changes in the torsion angle alone. Our results show that ~100% of the shielding change is due to torsion angle changes. The changes in bond lengths and angles that accompany the torsion angle changes in our work are very similar to those determined in the earlier work of Chesnut et al.,[21] as shown in Table 3, and thus the small difference in the relative magnitude of the torsional contribution may be attributed to an overestimation of the shielding derivative with respect to C–H bond length changes and the use of a smaller basis. We have also investigated *n*-octane, and once again we find that geometry optimization does not affect the torsional dependence of the shielding at the β-position.[22] This is a rather fortunate circumstance since geometry optimizations normally take about 10 times longer than an individual shielding calculation. Since we also show that nonoptimized peptide fragments permit excellent predictions of protein shielding in what follows, we only consider shielding calculations at various dihedral angles, while keeping the other geometrical parameters fixed. In addition to eliminating the time-consuming process of geometry optimization, the shielding traces we present here map only the changes in shielding that are a direct consequence of a change in a given torsion angle, and these appear to account very well for many experimental observations on proteins.

We next investigated shielding in two small hydrocarbons

Chart 1

propane	C_3H_8	$C^\beta HABC^\alpha HCD$	A = B = C = H; D = CH_3
2-methylpropane (isobutane)	C_4H_{10}	$C^\beta HABC^\alpha HCD$	A = B = H; C = D = CH_3

in which we use the substituted ethane designation system noted in Chart 1. Our shielding results as a function of χ^1, the $HC^\beta C^\alpha H$ torsion angle, are shown in Figure 2. Clearly, as expected, there is no change in the general shape of the torsional dependence of shielding for either C^β or C^α, but the sensitivity to χ^1 varies remarkably between the three systems studied. In particular, the relative C^α shielding (a CH_2 group) in propane as a function of χ^1 is large and essentially identical to the C^α shielding in isobutane (a CH group), and both are the same as in ethane (Figure 2A). However, the C^β or *methyl* group shieldings in ethane, propane, and isobutane vary greatly as a function of χ^1, as shown in Figure 2B. Apparently, alkyl substitution at C^α does not perceptibly influence the χ_1 dependence of shielding at C^α,

(22) de Dios, A. C.; Oldfield, E. Unpublished results.

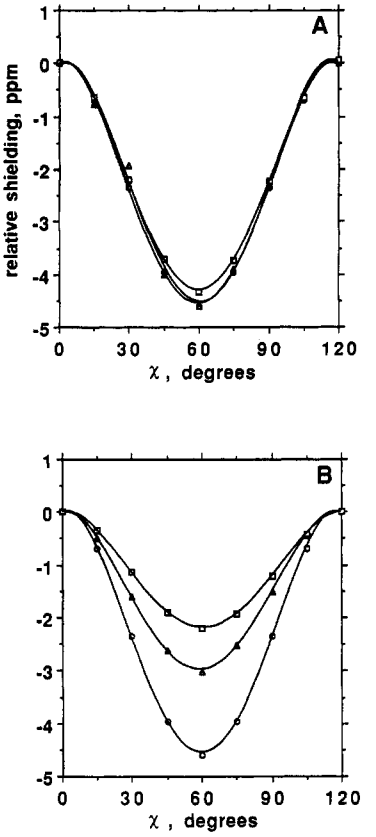

Figure 2. Calculated ^{13}C shieldings as a function of the torsion angle, χ, with increasing methylation: (A) C^α shielding of ethane (○), propane (△), and isobutane (□); (B) as in A but for (methyl) C^β.

but with C^β, increased alkyl substitution at C^α diminishes the χ^1 sensitivity (Figure 2B). As expected, for both C^α and C^β sites, the staggered conformations are deshielded with respect to the eclipsed conformations.

Now, since we are primarily interested in using chemical shifts to help interpret the structures of proteins, the next series of small molecules we investigated incorporated two key functional groups of importance in peptide structures: NH_2 and C=O. We investigate again C^β and C^α shielding in three model compounds (Chart 2).

Chart 2

aminoethane (ethylamine)	C_2H_7N	$C^\beta HABC^\alpha HCD$	A = B = C = H; D = NH_2
propanal	C_3H_6O	$C^\beta HABC^\alpha HCD$	A = B = C = H; D = CHO
(*S*)-2-aminopropanal (ϕ = –55°, ψ = 136)	C_3H_7ON	$C^\beta HABC^\alpha HCD$	A = B = H; C = NH_2; D = CHO

Addition of these highly polar residues to the ethane fragment results in a considerably larger range of shielding behavior as a function of χ^1 than with the alkanes (Figure 2), but there are also clear similarities. For example, the shielding functions all show a minimum in the vicinity of the staggered conformation. In addition, as found with the alkanes, shielding at the site of substitution (C^α) is uniformly larger in ethane, ethylamine, propanal, and 2-aminopropanal. For C^β, amino substitution in both ethylamine and 2-aminopropanal causes a greatly reduced χ^1 sensitivity, while CO substitution causes almost no effect at all—neither for C^α nor C^β (Figure 3A,B). In both Figures 2 and 3 there also appears to be a degree of transferability between the various shielding traces. For example, mono- and dialkyl substitutions cause decreased χ^1 sensitivity for the (C^β) methyl groups in propane and isobutane; amino substitution causes large C^α and C^β shielding sensitivity decreases, while carbonyl

Table 3. Torsion Effects on Energy, Bond Lengths, Bond Angles and ^{13}C Shielding in Ethane[a]

χ^1	R_{C-C} (Å)	R_{C-H} (Å)	∠HCH (deg)	E_{rel} (kcal/mol)	$\sigma(^{13}C)$ (ppm)	$\sigma(^{13}C_{rel})$ (ppm)
0°	1.5394 (1.5415)	1.0825 (1.0868)	107.24 (107.13)	2.971 (3.003)	190.96 (190.80)	4.61 (4.17)
60°	1.5254 (1.5276)	1.0836 (1.0877)	107.71 (107.64)	0.00 (0.00)	186.49 (186.14)	0.00 (0.00)
diff	0.0140 (0.0139)	−0.0011 (−0.0009)	−0.47 (−0.51)		4.47 (4.66)	

[a] Values in parentheses were obtained from ref 21.

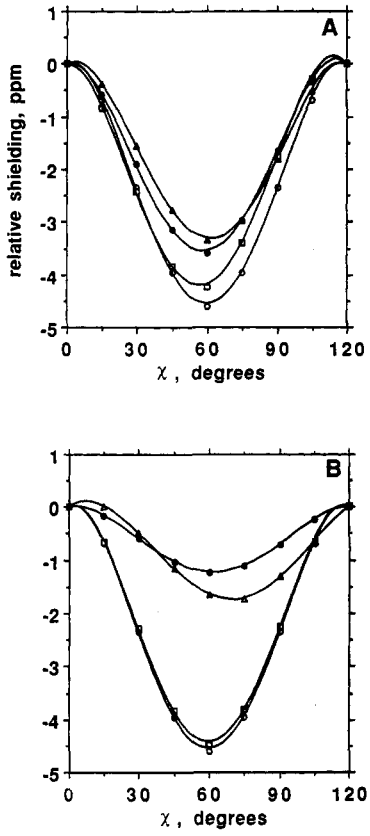

Figure 3. Calculated ^{13}C shieldings as a function of the torsion angle, χ, with different C^α substituents: (A) C^α shielding of ethane (○), ethylamine (△), propanal (□), and 2-aminopropanol (●); (B) as in A but for (methyl) C^β.

substitution has little effect in ethylamine, propanal, and 2-aminopropanal, but such conclusions need to be drawn carefully since, as we will discuss below, this transferability turns out to be present only when substitution occurs at a single carbon. Given these simple "benchmark" model compound calculations, we thus move on to consider the ϕ, ψ, and χ^1 torsional contributions to shielding in two more complex ethane derivatives:
formylalanine amide

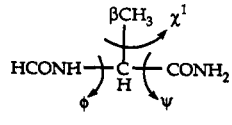

$C_4H_8O_2N_2$ $C^\beta HAB\ C^\alpha HCD$ A=B=H; C = NHCHO; D = $CONH_2$

and formylvaline amide

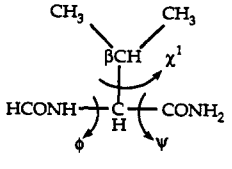

$C_6H_{12}O_2N_2$ $C^\beta HAB\ C^\alpha HCD$ A=B=CH_3; C = NHCHO; D = $CONH_2$

Here, we again need to briefly consider the topic of the appropriate geometries to be used—is optimization needed? *Ab initio* geometry optimization for the purpose of modeling peptides is still in its infancy (see, for example, ref 23), and in recent work, it has been shown that the "dipeptide approximation" is inadequate. For example, in terms of energy, one need only cite the fact that the helical conformation is not an energy minimum in a dipeptide space. Moreover, variations in backbone bond angles and bond lengths are observed when neighboring peptides are incorporated into the geometry optimization. Thus, in order to do an adequate geometry optimization, one needs to consider an oligopeptide with at least five residues—a very lengthy calculation. However, if geometry optimization is unnecessary, calculations of shielding surfaces such as the ones presented below would no longer be prohibitive. Fortunately, there are clear indications that this is the situation. *First*, we have already examined how the chemical shift is affected by geometrical factors other than torsion angles,[8] and it is apparent from our previous studies on glycine, alanine, and valine residues that the chemical shift nonequivalencies observed for the C^α shielding in proteins are dominated by torsion angle contributions.[3,4,8,24] Thus, the experimental chemical shifts are reproduced simply by taking into account the changes in shielding which come directly from torsion angle variations, without considering any changes in the other geometrical parameters that may accompany changes in torsion angle. *Second*, we note that ϕ,ψ shielding surfaces obtained for C^α in glycine obtained with and without geometry optimization are very similar. Figure 4A shows a plot of C^α shielding in a glycine fragment using an optimized geometry[25] (with a small basis) *versus* our standard fragment (GIAO/6-311++G(2d,-2p)), taken over the entire ϕ,ψ surface (rmsd = 0.81 ppm), while Figure 4B shows computed C^α shifts for the glycine residues in calmodulin and *Staphylococal* nuclease (rmsd = 0.16 ppm). Clearly, in allowed regions of ϕ,ψ space, there is essentially no difference between the results obtained.

We have thus used standard geometries, rather than "optimized" ones, since (1) at least for glycine C^α there is little difference upon optimization and (2) inter-residue[23] and correlation effects are likely to be important in optimizations, and optimization of, for example, a valine-containing pentapeptide at the correlated wave function level is expected to be not only lengthy but, based on our success in reproducing Gly, Ala, and Val shieldings in proteins using unoptimized geometries, unnecessary.

Formylalanine amide might be expected to have a χ^1 shielding dependence rather similar to that seen with 2-aminopropanal, since the only structural differences between the two molecules are the additional substitutions $NH_2 \rightarrow$ HCONH and CHO → $CONH_2$. However, the presence of two highly polar (peptide) groups could also well introduce a very major additional ϕ,ψ effect (as we have indeed noted elsewhere, see e.g. refs 3 and 8) which needs to be investigated.

We show in Figure 5A the χ^1 dependence of C^α shielding in formylalanine amide at four different ϕ,ψ torsion angles. Interestingly, the χ^1 dependence of the C^α shielding shown in Figure 5A does not seem to be influenced by the torsion angles ϕ and ψ, with all traces showing a minimum near the staggered conformation. Moreover, the χ^1 dependence shown in Figure 5A is very comparable to that seen with 2-aminopropanal (Figure 3A).

The helix/sheet 1 model compound shielding separation for

(23) Schaefer, L.; Newton, S. Q.; Cao, M.; Peeters, A.; Van Alsenoy, C.; Wolinski, K.; Momany, F. A. *J. Am. Chem. Soc.* **1993**, *115*, 272.
(24) Pearson, J. G.; Le, H.; de Dios, A.; Oldfield, E. Unpublished results.
(25) Jiao, D.; Barfield, M.; Hruby, V. J. *J. Am. Chem. Soc.* **1993**, *115*, 10883.

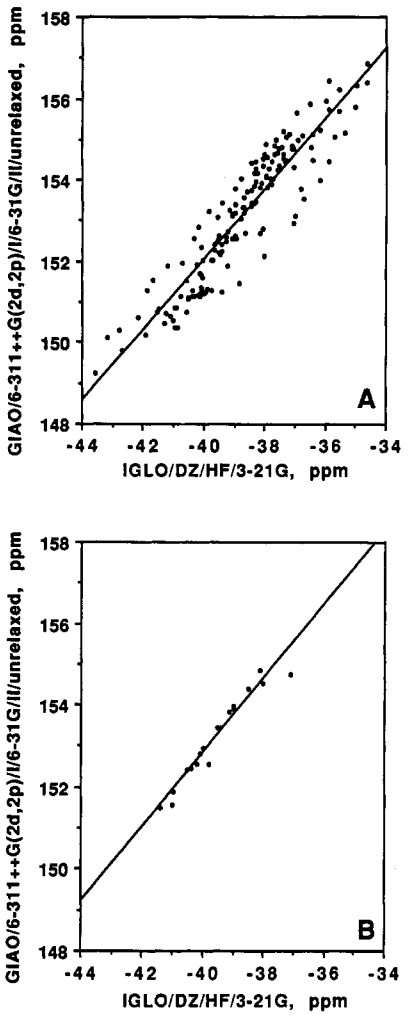

Figure 4. Comparison between C^{α} shieldings computed using IGLO with optimized geometries (ref 25) and GIAO with standard fragment geometries (ref 4): (A) data sampled over the entire ±180° ϕ,ψ region of Ramachandran space (rmsd = 0.81 ppm); (B) data points corresponding to allowed regions of ϕ,ψ space as exemplified by the glycine C^{α} sites in calmodulin and *Staphylococcal* nuclease (rmsd = 0.16 ppm).

C^{α} is ~4.3 ppm, a typical value found in proteins. For example, in *Staphylococcal* nuclease, the *maximal* alanine C^{α} shift range is ~6.3 ppm,[26] which is overwhelmingly dominated by ϕ,ψ torsional effects—although, as reported previously, hydrogen bonding and longer range electrostatic field effects (which may be indirectly ϕ,ψ related) account for a further 1–2-ppm shielding contribution.[3] On the basis of the SCF energies, the rotational barriers in the alanine helix and sheet models are 4.3 kcal mol^{-1} and 4.6 kcal mol^{-1}, respectively, in general accord with methyl group activation barriers of ≈4 kcal mol^{-1} determined for crystalline alanine *via* solid-state NMR.[27]

The C^{β} site presents a much more unusual picture of χ^1 shielding dependence as shown in Figure 5B, where it can be seen that the shielding does not have its maximum value at the eclipsed (0°) conformation. In addition, the χ^1 dependence is strongly dependent on ϕ and ψ, and especially at positive ϕ,ψ, the shielding function no longer has an extremum in the vicinity of the staggered conformation (60°). This is all the more surprising since none of these features are present in the potential energy surface, where the ~4–5-kcal methyl rotation barrier has a minimum at 60° and a maximum value at 0°.

(26) Torchia, D. A.; Sparks, S. W.; Bax, A. *Biochemistry* **1988**, *27*, 5135. Torchia, D. A.; Yamazaki, T. Private communication.
(27) Keniry, M. A.; Kintanar, A.; Smith, R. L.; Gutowsky, H. S.; Oldfield, E. *Biochemistry* **1984**, *23*, 288.

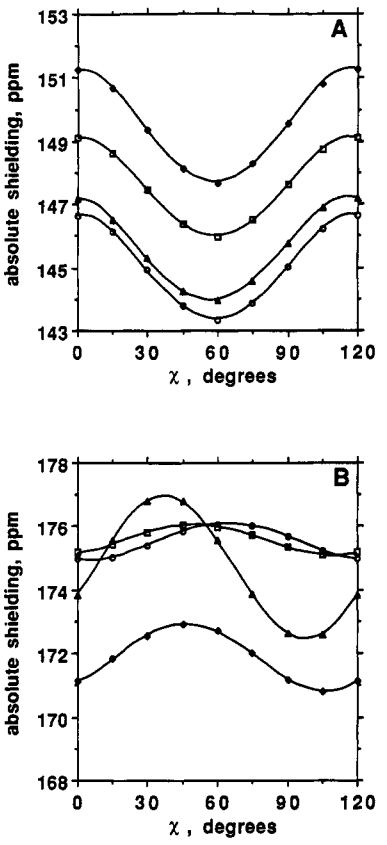

Figure 5. Calculated ^{13}C shieldings as a function of the torsion angle, χ, for an alanine model fragment at different ϕ and Ψ angles: (A) C^{α} shielding for helix (ϕ = –58, Ψ = –51) (○), turn (ϕ = 55, Ψ = 50) (△), sheet 1 (ϕ = –140, Ψ = 140) (◇), and sheet 2 (ϕ = –71, Ψ = 140) (□); (B) as in A but for (methyl) C^{β}.

We also find that the comparison of the calculated shielding values with experiment for C^{β} is much less ideal than with C^{α}. For example, for the same protein (*Staphylococcal* nuclease), the total chemical shift range[26] is found to be 7.8 ppm (Ala^{109} = 25.6 ppm (ϕ = –163, ψ = 153), Ala^{130} = 17.8 ppm (ϕ = –62, ψ = –42)), while from Figure 5B, it can be seen that the difference between the helix and sheet 1 fragments at the staggered conformation is only 3.3 ppm, less than one-half of what is observed experimentally. Once again, as with C^{α}, the chemical shift difference between sites in sheet and helical conformations cannot be significantly increased by averaging over χ^1. One can see from Figure 5B that the largest difference between these two conformations is about 5 ppm, and this already involves a sheet residue at the eclipsed conformation and a helical fragment at a staggered one.

The C^{β} site differs from C^{α} in two ways. First, C^{β} lies at a γ-position with respect to the angles ϕ and ψ, and as mentioned earlier, Webb et al.[16] found additional changes in shielding of the atom in a γ-position caused by changes in bond angles and bond lengths which accompany the change in the dihedral angle. However, we find that full relaxation of the other parameters at a given pair of ϕ and ψ angles leads to a 12% reduction in shielding difference for C^{β} in sheet and helical residues (data not shown). The second difference may be related to the influence of the "other" effects noted in eq 1, i.e. the influence of σ_e and σ_m on C^{β} shielding, and indeed, in previous work on *Staphylococcal* nuclease in which we incorporated explicitly the effects of hydrogen bonding and electrostatics, we were able to successfully account for the observed chemical shift dispersion.[3] In order to explore this topic further, we have thus investigated the likely long-range contributions to shielding in a series of small peptide molecules—to see for example how i + 1, i + 2, etc., residues contribute to shielding. For very large (heptapeptide) fragments,

Table 4. Calculated Alanine C^β Shieldings (ppm) for Peptides of Increasing Size[a]

molecule	helix	sheet
HCO-Ala-NH_2	189.9	185.5
HCO-Gly^3-Ala^4-Gly^5-NH_2	189.9	185.8
HCO-Gly^2-Gly^3-Ala^4-Gly^5-Gly^6-NH_2	190.7	185.8
HCO-Gly^1-Gly^2-Gly^3-Ala^4-Gly^5-Gly^6-Gly^7-NH_2	191.1	185.8

[a] The exact conformations are given in Table 2.

Table 5. Torsion Angles and Chemical Shifts for Valine Residues in *Drosophila melanogaster* Calmodulin

residue	ϕ (deg)[a]	ψ (deg)[a]	χ^1 (deg)[a]	C^α (ppm)[b]	C^β (ppm)[b]
35	−64	−49	174	66.1	31.3
55	−102	−21	−41	61.0	32.7
91	−70	−37	48	65.7	31.5
108	−63	−34	−39	66.1	31.7
121	−68	−40	169	67.1	31.4
136	−114	125	−29	61.8	33.6
142	−65	−39	−40	67.3	31.4

[a] Reference 28. [b] Reference 26.

there is of course a conflict between basis size and fragment size. Thus, we chose to explore only C^β shielding in the larger species since use of a uniform (6-31G) basis can be expected to be adequate for a CH_3 group, and on the basis of the results discussed above (and below), the only anomalous effect is found with alanine C^β. The results of the C^β shielding calculations for peptides of increasing size are listed in Table 4. It can be seen that the C^β shielding for a sheetlike conformation does not change appreciably as one increases the size of the fragment, while the helical fragments behave quite differently, with the heptapeptide being 1.2 ppm more shielded than the monomer. The remaining 2–3-ppm shielding difference between theory and experiment presumably comes from longer range electrostatic field effects (possibly including hydrogen bonding), and in previous work,[3] we have shown that the complete shielding pattern for *Staphylococcal* nuclease can be well reproduced using the GIAO approach, with charge-field perturbation.[3]

From the standpoint of actually predicting protein ϕ,ψ torsion angles from C^α, C^β chemical shifts, it would appear that the method could be jeopardized by the difficulties associated with C^β shift predictions using the shielding surface approach. However, we have recently found that the electrostatic/hydrogen bonding "other" non-ϕ,ψ contributions to shielding are in fact correlated with ϕ,ψ. Thus, we find a 0.91 correlation coefficient between predicted and experimental C^β shifts[24]—excellent agreement, even though the slope is only 0.62.[24] While basis deficiencies alone might be the cause of this decreased slope, the observation that hydrogen bonding and charge-field perturbation do indeed permit accurate prediction of C^β shifts[3] suggests that these are the major origins of the decreased slope. In addition, the observation that the predictions for C^α (expected to require an even larger basis) are accurate[3] also implies a significant ($\sigma_e + \sigma_m$) contribution for alanine C^β. These effects can be handled semiempirically,[24] and we have recently found it possible to predict protein ϕ,ψ values to $\sim 10°$ using solely "calibrated" C^α, C^β, and experimental H^α shielding surfaces.

In all the molecules we have studied so far, only the carbon at the α-position has substituents other than hydrogen. For amino acids, however, β-substitution might be expected to cause a large change in the χ^1 dependence of shielding at both the α- and β-positions, since a β-substituent reduces the symmetry. Thus, the staggered conformations (at $\chi^1 = 60°$, $-60°$, and $180°$) are now unique, and both potential and shielding curves will become more sensitive to χ^1 due to the presence of bulky groups at both α- and β-positions. We have thus computed the shielding of C^α and C^β in a valine model fragment as a function of χ^1, for a range of representative ϕ and ψ angles. Although the model we use here for a sheet residue has ϕ and ψ angles similar to the ones

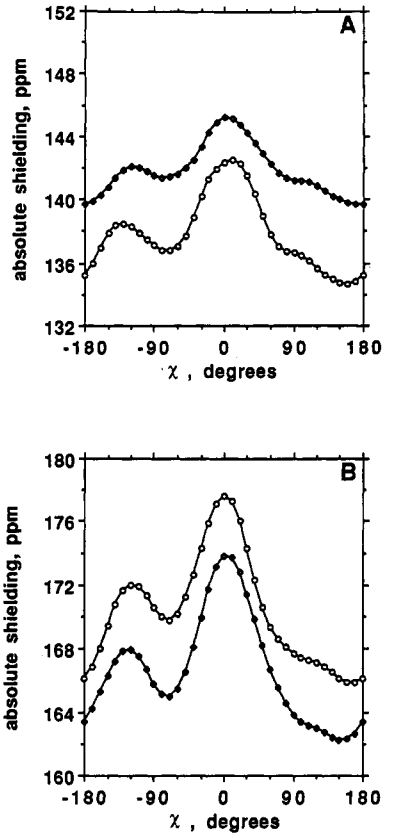

Figure 6. Calculated ^{13}C shieldings as a function of the torsion angle, χ, for a valine model fragment at different ϕ and Ψ angles: (A) C^α shielding for helix ($\phi = -55$, $\Psi = -55$) (○) and sheet ($\phi = -136$, $\Psi = 143$) (◇); (B) as in A but for C^β.

previously reported,[8] the bond lengths and bond angles for the fragment used in the present work are from optimized values (at $\chi^1 = 180°$); hence, the absolute values are slightly different. The results for the valine model fragment are displayed in Figure 6. As predicted, both C^α (Figure 6A) and C^β (Figure 6B) show a shielding value for the *trans*-conformation, $\chi^1 = 180°$, that is different from the values at the *gauche*-conformations, an example of a "vicinal *gauche*" effect.[18] The effect is substantial, about 4 ppm, especially for C^β in the helical conformation, with the *gauche*-conformer being more shielded. This difference is large enough to be useful in determining side chain conformations of valine residues in proteins, provided that ϕ and ψ angles are known. The two *gauche*-conformers do not show significantly different shieldings, although with stereospecifically assigned C^γ it appears to be possible[22] to distinguish between $\chi^1 = 60°$ and $\chi^1 = -60°$. The increase in the overall shielding range for the valine fragment is evident for both carbons, especially the dramatic change in sensitivity of C^β shielding to χ^1, which now has a range of 10 ppm. For both carbon shieldings, the deviation from the shape of the potential curve is also noticeable; in particular, there is no extremum at the vicinity of $\chi^1 = 60°$.

For valine residues, we find a significant (*anti*) correlation between experimental C^α and C^β chemical shifts ($R = 0.74$; in *Staphylococcal* nuclease[26] and a vertebrate calmodulin[28]), and this behavior is reflected in the C^α and C^β shielding traces for both helical and sheet fragments, as shown in Figure 6A,B. Figure 6A,B shows that the apparent *anti*-correlation between C^α and C^β chemical shifts most probably comes from the ϕ and ψ dependencies. As can be seen from Figure 6, C^α is deshielded in a helical conformation while a helical C^β is shielded, in general

(28) Ikura, M. Private communication. Ikura, M.; Spera, S.; Barbato, G.; Kay, L. E.; Krinks, M.; Bax, A. *Biochemistry* **1991**, *30*, 9216.

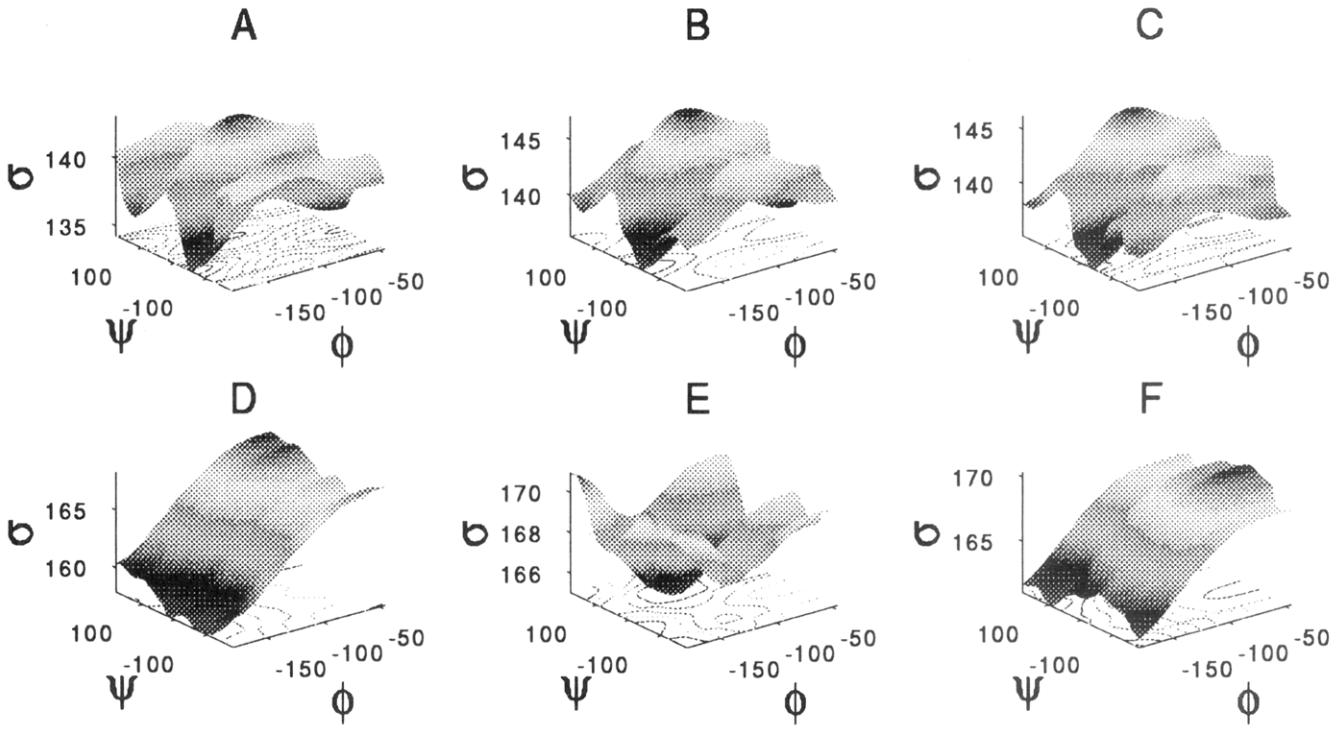

Figure 7. Calculated $^{13}C^{\alpha}$ and $^{13}C^{\beta}$ shieldings in formylvaline amide as a function of ϕ and ψ (at various χ^1 values): (A) C^{α}, $\chi^1 = 180°$; (B) C^{α}, $\chi^1 = 60°$; (C) C^{α}, $\chi^1 = -60°$; (D) C^{β}, $\chi^1 = 180°$; (E) C^{β}, $\chi^1 = 60°$; (F) C^{β}, $\chi^1 = -60°$.

accord with the empirical results of Spera and Bax.[29] The dominance of ϕ and ψ in the chemical shift nonequivalencies of C^{α} and C^{β} nuclei of valine residues in proteins is, however, quite unexpected given the observation that, in the X-ray structure of, for example, calmodulin,[30] there are a wide variety of χ^1 angles, which would be expected to destroy any correlation. This apparent discrepancy is even more noticeable when the range of C^{β} shifts is considered: five out of the seven valine residues in calmodulin (Val^{35}, Val^{91}, Val^{108}, Val^{121}, and Val^{142}) have C^{β} resonances at 31.3–31.7 ppm (a range of only 0.4 ppm), while the X-ray structure shows vastly different χ^1 angles (Table 5). There would seem to be two possible explanations for these observations: *First*, the other ($\sigma_e + \sigma_m$) interactions could all conspire in such a way as to reduce the C^{β} shielding range to 0.4 ppm. *Second*, it is possible that these five residues all in fact have very similar ϕ, ψ, and χ^1 torsion angles, and there is actually a significant difference between the χ^1 populations in solution and the crystalline solid state. On the basis of the result of the calculations presented in Figure 6 and after taking into account the fact that the above five residues all have helical ϕ and ψ angles *and* very similar C^{α} and C^{β} shifts, the most likely solution would seem to be that all five residues are either all *trans*-conformers or all *gauche*-conformers in solution.

To test this hypothesis further and determine if a single χ^1 angle predominates, one needs to evaluate C^{α} and C^{β} shifts in terms of an absolute shielding scale. As stated earlier, from Figure 6, the valine *gauche*-conformers are about 3–4 ppm more shielded than the *trans*-conformers, for both C^{α} and C^{β}. It should thus be possible to use a comparison with other sites, such as C^{α} and C^{β} of alanine, to properly position the absolute shieldings of C^{α} and C^{β} nuclei in valine sites. Then, with a knowledge of the shielding dependence of C^{α} and C^{β} on ϕ and ψ, evaluation of the absolute shieldings in valine residues can be achieved. Since there are three likely χ^1 conformers, we thus need to evaluate C^{α} and C^{β} shieldings as a function of ϕ,ψ and generate shielding surfaces $\sigma(\phi,\psi,\chi^1)$. We then use alanine C^{α}, C^{β} shielding surface results to correctly place valine C^{α}, C^{β} shieldings on an absolute scale (since alanine has no significant χ^1 dependence at room temperature). Of course, ideally, one should generate a full hypersurface dependent on all χ_1. However, this would be very computationally demanding. We have thus computed the six ϕ and ψ shielding surfaces for the C^{α} and C^{β} sites in valine at the three different conformations, $\chi^1 = 180°$, 60°, and –60°, and these are illustrated in Figure 7. Figure 7A–C corresponds to shielding of the C^{α} nucleus while the bottom row (Figure 7D–F) is for C^{β}. Each surface is for a particular χ^1 conformer: the first column is for the *trans*-conformer ($\chi^1 = 180°$) while the second and third columns correspond to the *gauche*-conformers ($\chi^1 =$ 60° and –60°, respectively). The following shows the structure of each fragment:

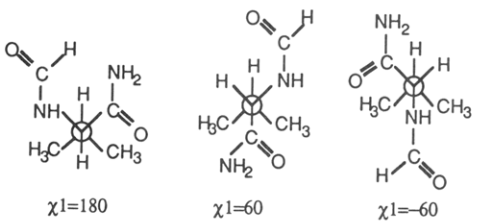

It is obvious from Figure 7 that, except for the shift in absolute values, the ϕ and ψ dependencies of C^{α} are very similar in all three conformers. This is not unexpected given the traces shown in Figure 6A, where the two curves to a first approximation track each other very closely throughout the whole range of χ^1. In contrast, in Figure 6B (the C^{β} χ^1 shielding traces), it can be seen that the two curves approach each other very closely at $30° < \chi^1 < 60°$ such that the difference between the helical and sheet C^{β} shieldings in this region are at a minimum. The bottom (C^{β}) row of surfaces shown in Figure 7 agrees well with these observations. Thus, the left and right surfaces ($\chi^1 = 180°$ and –60°) are very similar, while the surface in the center ($\chi^1 = 60°$) shows a quite different shape. It has a minimum in the vicinity of $\phi = -126°$ and $\psi = 54°$, and the contours are concentric about this point. As a result, the sheet ($\phi = -136°$ and $\psi = 143°$) and helical ($\phi = -55°$ and $\psi = -55°$) conformers do not differ greatly from one another. This uniqueness of the ϕ–ψ shielding surface

(29) Spera, S.; Bax, A. *J. Am. Chem. Soc.* **1991**, *113*, 5490.
(30) Chattopadhyaya, R.; Meador, W. E.; Means, A. R.; Quiocho, F. A. *J. Mol. Biol.* **1992**, *228*, 1177.

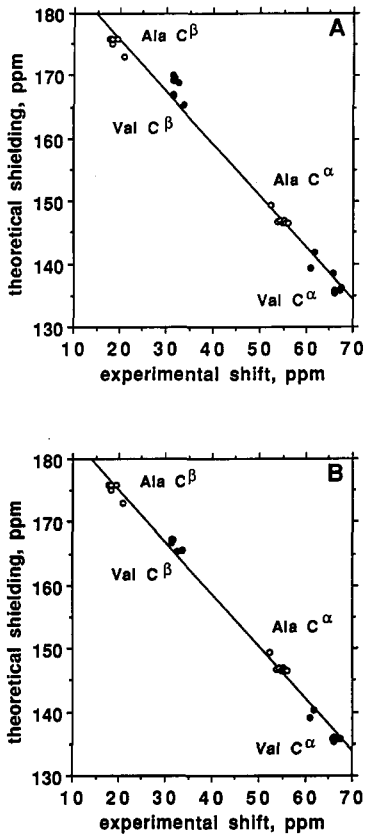

Figure 8. Calculated $^{13}C^{\alpha}$ and $^{13}C^{\beta}$ shieldings for alanine (○) and valine (●) residues in calmodulin: (A) using the torsion angles derived from the X-ray structure,[30] the shielding surfaces shown in Figure 6 for valine, and the alanine shielding surfaces reported in ref 8; (B) as in A but a χ^1 of 180° is assumed for all valine residues. The experimental chemical shifts are given in ppm from TSP (ref 26).

at $\chi^1 = 60°$ appears to originate from the relative position of the C^{α}–C^0 bond with respect to the γ-CH_3 groups, as shown by the conformers above. In this conformation, the C^{α}–C^0 bond lies between the two methyl groups and may lead to an enhanced sensitivity of the C^{β} shielding on the dihedral angle ψ(N–C^{α}–C^0–N). For $\chi^1 = 180°$ and –60°, the C^{α}–C^0 bond lies between H^{β} and a γ-methyl, and the two shielding surfaces are quite similar (Figure 7D,F).

From the shielding surfaces shown in Figure 7, one can predict the shieldings for C^{α} and C^{β} provided the angles ϕ and ψ are known. Using the angles derived from the X-ray structure of calmodulin[30] and the shielding surfaces shown in Figure 7, the C^{α} and C^{β} shieldings for valine sites can be determined, and these are shown in Figure 8A. The theoretical shielding values are plotted against the experimental shifts of Ikura,[28] and also included in this plot are the theoretical values for the alanine sites in the same protein derived from the shielding surfaces reported previously.[8] It can be seen that the shielding differences among the valine points are overestimated, and as suggested earlier, the greater chemical shielding dispersion may be due to the valine residues existing in conformations different from those reported in the X-ray structure. To explore this further, in Figure 8B, a *trans*-conformation ($\chi^1 = 180°$) has been assumed for all sites, and this clearly results in a decrease in the theoretical shielding dispersion and a substantial decrease in the deviation of the valine points from the fitted curve (the rmsd decreases from 2.7 to 1.6 ppm when $\chi^1 = 180°$ is assumed for all valine sites). The *trans*-conformation is also favored because the *gauche*-conformers lead to more shielded values, which brings the valine points farther from the fitted curve. On the basis of this protein, an absolute shielding of 166 ppm corresponds to a chemical shift of about 31.5 ppm with respect to (trimethylsilyl)propionic acid (TSP). If this view is correct, then it can be expected that a helical valine site that gives a C^{β} chemical shift of 31 ppm from TSP has a χ^1 of 180°. The other conformers will give C^{β} chemical shifts of about 27 ppm.

Of course, the above arguments would be strengthened if there were independent evidence as to the nature of χ^1 *in solution.* Fortunately, the chemical shift is not the only observable that can be used to deduce the side chain conformations of these valine residues, and although more difficult to measure compared with chemical shifts, the three-bond proton–proton scalar coupling constant, $^3J_{H^{\alpha}H^{\beta}}$, is also dependent on χ^1. A maximum value of this coupling constant is expected at $\chi^1 = 180°$, thereby differentiating it from the other conformations. Upon the basis of coupling constant information obtained from Ikura,[28] six out of the seven valine residues (Val^{35}, Val^{91}, Val^{108}, Val^{121}, Val^{136}, and Val^{142}) have large values for $^3J_{H^{\alpha}H^{\beta}}$, indicative of $\chi^1 = 180°$, in complete agreement with the conclusions that we derived solely from chemical shift information. Val^{55} exhibits only a medium value for this coupling constant. In a closely-related system, calmodulin complexed with a 26-mer peptide, Vuister and coworkers[31] have used heteroatom three-bond couplings $^3J_{C^{\gamma}N}$ and $^3J_{C^{\gamma}C^0}$ in determining the side chain conformation of valine residues in calmodulin, and their conclusions are the same as the ones we derive for the uncomplexed species. Out of the seven residues, only Val^{55} does not have a χ^1 at 180°, and apparently, this residue undergoes rotamer averaging. Our chemical shift analysis, however, implies that the *trans*-conformer predominates here also.

Acknowledgment. We thank Professors P. Pulay and J. F. Hinton and Dr. K. Wolinski for providing us with a copy of their TEXAS program, Drs. D. Torchia and M. Ikura for sharing with us their experimental results, and Professors C. J. and A. K. Jameson for helpful advice.

(31) Vuister, G. W.; Wang, A. C.; Bax, A. *J. Am. Chem. Soc.* **1993**, *115*, 5334.